Multi-anode Detection in Electrospray Ionization Time-of-Flight Mass Spectrometry

D. C. Barbacci and D. H. Russell
Department of Chemistry, Texas A&M University, The Laboratory for Biological Mass Spectrometry, College Station, Texas, USA

J. A. Schultz, J. Holocek, S. Ulrich, W. Burton, and M. Van Stipdonk
IonWerks, Inc., Houston, Texas, USA

An electrospray ionization ion source coupled to a time-of-flight mass analyzer incorporating a multi-anode time-to-digital converter is described. High-speed data acquisition (kHz mass spectral acquisition) rates are achieved. The four-anode detector produces a significant increase in detection/counting efficiency over that for a single-anode detector. In this work a 2.5 times increase in detection efficiency is demonstrated. The multi-anode detector is also used as a diagnostic tool to optimize transmission of the ion optics. (J Am Soc Mass Spectrom 1998, 9, 1328–1333) © 1998 American Society for Mass Spectrometry

Liquid chromatography mass spectrometry (LC-MS) is a powerful method for identification and structure elucidation of complex organic and biological compounds. The recent developments in electrospray ionization (ESI) clearly demonstrate the potential of ESI as an analytical method for analysis of biological compounds [1, 2], but the spectral congestion because of the distribution of charge states limit the utility for mixture analysis [3]. Consequently, the development of ESI-LC-MS is of critical importance for the optimum use of ESI for process analysis, especially for process analysis of complex mixtures.

ESI-MS has traditionally used quadrupole mass analyzers to couple the continuous output of the ESI with the analyzer. The quadrupole is particularly suited to ESI because the continuous flow of the ESI can be directly introduced. However, the available mass range, the scan time (milliseconds per decade of mass-to-charge ratio), and the mass resolution impose impediments to the full utilization of the method. Clearly, the problems associated with the limited mass-to-charge ratio range are less critical for the analysis of compounds that yield high charge states. But, the analysis of proteins in a nondenaturing solution and near physiological pH conditions will result in mass-to-charge ratio values that exceed the mass range of the quadrupole analyzer [4, 5].

Recently, time-of-flight (TOF) mass analyzers have been couple to ESI sources [6, 7]. The major advantage of the TOF analyzer is the unlimited mass-to-charge ratio range, the acquisition of a complete mass spectrum for each pulsed ion extraction event (e.g., the so-called Fellegett advantage), high resolution and accurate mass measurements. The greatest impediments to the development of ESI-TOF and ESI-LC-TOF are the requirements of pulsed ion extraction and limitations in the data acquisition [8]. Currently, the data acquisition system most suited to meet the requirements of ESI-TOF is time-to-digital conversion (TDC). For example, TDC's are fast and capable of high-resolution measurements. Furthermore, mass resolution obtained by using a TDC is not dependent on detector response but instead depends on leading edge of the signal. The limitation of the TDC is that only one count is registered per simultaneous event on the detector. That is, the signal recorded is not proportional to the number of ions simultaneously arriving at the detector plane. The capabilities of the latest technology TDC data acquisition systems are truly examples of time-array detectors [9]. The memory storage allows 256k and higher data bins for high resolution and long acquisition times in the same spectrum. In addition, the number of stop events per acquisition cycle has also increased allowing for late arriving ions to be detected.

To circumvent low counting efficiency in TDC acquisition systems, multiple anodes, or so-called multipixel detectors can be placed behind the microchannel plate (MCP) detector. The presence of multipixel anodes allows for the possibility of multiple simultaneous ion arrival to be counted. In this paper we present experimental results of the implementation of a four-anode detector for TDC acquisition. The four-anode device is tested for sensitivity and resolution.

Experimental

The ESI-TOF instrument is a PerSeptive Biosystems Mariner alpha version (PerSeptive Biosystems, Fra-

Address reprint requests to D. H. Russell, Department of Chemistry, Texas A&M University, The Laboratory for Biological Mass Spectrometry, College Station, TX 77843. E-mail: Russell@chemvx.tamu.edu

1044-0305/98/$19.00
PII S1044-0305(98)00113-5

Received March 16, 1998
Revised August 7, 1998
Accepted August 7, 1998

mingham, MA) and is similar to the instrument described by Verentchikov et al. [7]. The ESI source consists of three stages of differential pumping. The spray is produced at atmosphere with a countercurrent flow of nitrogen gas. The spray enters a narrow hole of a heated capillary (nozzle) into a region that is backed by a Leybold D30 (27 CFM) mechanical pump operating at a pressure of approximately 2 torr. The spray then passes through the first skimmer into a region backed by an Alcatel M2012A (11 CFM) mechanical pump operating at a pressure of 50–100 mtorr. The third stage is evacuated with a Pfeiffer Balzer TPH 240 (230 L/s) turbomolecular pump and operates at approximately 10^{-5} torr. Ions pass through a 1.5 mm by 10 mm aperture to the orthogonal extraction TOF region. The TOF region is evacuated with Pfeiffer Balzers TPH 240 turbomolecular pump and operates at a background pressure of 5×10^{-7} torr. Both turbomolecular pumps are backed with the same Precision DD 310 (11 CFM) mechanical pump. Liquid flow is 1.34 μL/min unless otherwise stated. The spray voltage was 2.8 kV (Spellman model RHSR5PN50X1884, Plainview, NY) and the needle to nozzle distance was approximately 3 mm. The nozzle, skimmer 1, and skimmer 2 voltages were set at 125, 40, and 30 V, respectively. The orthogonal extraction region is operated from ground potential. The TOF is initiated with a 400 V (Bertan model 603C-15P, Hicksville, NY) positive voltage pulse on the push plate and a 200 V negative (Bertan model 602C-15N) voltage pulse on the pull plate. The positive and negative pulsing circuits were built in-house. The digital delay generator controls the initialization and width of the positive and negative pulses. Ions are accelerated to −3750 V (Spellman model RHSR10PN60) and drift in a field free region held at −3750 V. The drift region is approximately 0.7 m. The ion mirror is operated at a potential difference of 7000 V, −3750 to 3250 V (Spellman model RHSR5PN50X1885). The length of the mirror is 0.197 m. The front of the microchannel plates (chevron assembly) is biased at the drift tube voltage. The anode is held at approximately −1650 V and is connected to a high voltage supply (Bertan model 323) through a resistor so that the gain of the detector may be varied without affecting the TOF region.

The multi-anode detector and multichannel TDC were developed for use with current amplifier, discriminator technology. The multi-anode is a four-anode design. The common flat anode is partitioned into quadrants. Each quadrant is electrically isolated from the other three and each quadrant is equipped with an output connection. The four outputs are connected to four vacuum feedthroughs, then to four amplifier channels (EG&G model FTA 820A, Oak Ridge, TN) with a gain of 200 per channel. After the amplifier the signal is sent to four discriminator channels (Phillips Scientific model 708, Ramsey, NJ) where the level was set to 700 mV, and to four TDC channels (Ionwerks model TDCx4, Houston, TX). The output pulse width of the discriminator was set to 3 ns. The pulsed extraction and data analysis are simultaneously triggered with a digital delay generator (EG&G PAR model 9650, Princeton, NJ). Pulse duration is 10 μs and TOF analysis is 100 μs unless otherwise noted. The acquisition rate was 9000 Hz and acquisition time was 600 s unless otherwise noted.

A multichannel, multihit high resolution TDC (Ionwerks model TDCx4) was used to measure ion flight times. The unit accepts standard fast timing signals from up to four inputs simultaneously (e.g., the four discrete anodes) and processes them in parallel with a time-digitizing resolution of 780 ps. The worst case pulse pair resolution within a single channel was 24 ns. Recording times were adjustable, ranging from 3 to 800 μs in 3 μs steps. The unit includes an on-board dual port buffer memory that held the timing of at least 2000 events for no-deadtime data recording. Data were histogrammed in hardware, and transferred from histogram memory to the host computer via a programmed I/O board.

To compare the four-anode detector to a single-anode detector the four signal outputs were connected to make one signal output. The single signal output was connected to one of the four amplification/discrimination/TDC channels used in the four-anode configuration and the same gain/discrimination level/TDC counting parameters from the four-anode configuration were used for the single-anode configuration measurements.

The same microchannel plates (Galileo Electro-

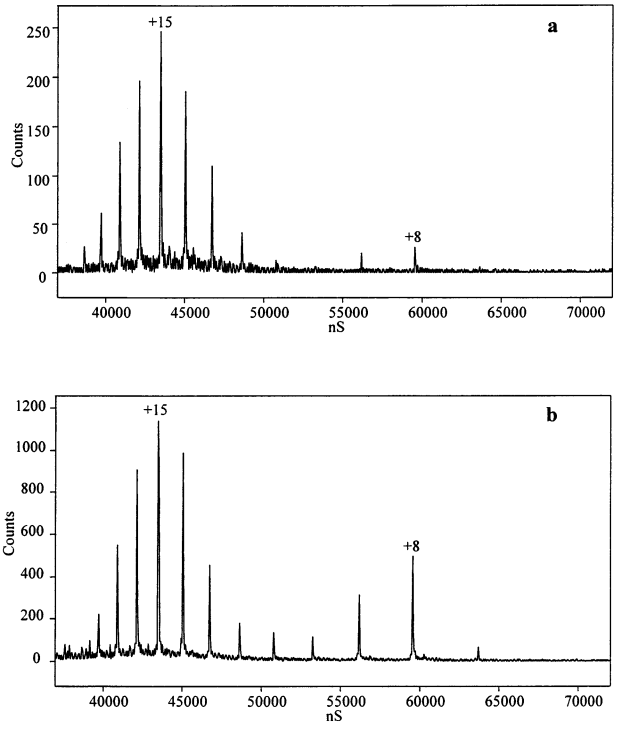

Figure 1. Time spectrum of cytochrome *c* (0.2 μM) acquired at 9 kHz for 600 s with **(a)** single-anode and **(b)** four-anode detector.

Table 1. Integrated area of observed charge states of cytochrome *c* at 0.2 μM

Single anode	Area (Counts * nS)							
Charge state	Trial 1	Trial 2	Trial 3	Trial 4	Trial 5	Average	Std. Dev.	CV
+19	478	369	311	333	473	**393**	**78**	**19.9**
+18	1800	1287	1141	758	1236	**1244**	**373**	**30.0**
+17	3053	2550	3219	2944	2917	**2937**	**247**	**8.4**
+16	5037	3644	4394	4894	5148	**4623**	**619**	**13.4**
+15	6225	5206	6052	5597	6081	**5832**	**422**	**7.2**
+14	5706	3959	5294	5173	5241	**5075**	**657**	**13.0**
+13	2137	2269	3183	2697	2537	**2565**	**410**	**16.0**
+12	612	580	644	746	692	**655**	**66**	**10.0**
+11	216	185	172	220	161	**191**	**26**	**13.8**
+10		180	81	66	137	**116**	**52**	**45.2**
+9	400	173	275	255	325	**286**	**84**	**29.5**
+8	494	358	397	334	502	**417**	**77**	**18.5**
	26158	**2760**	**25163**	**24017**	**25450**	**24310**	**2129**	**8.8**
Four anode	Area (Counts * nS)							
Charge state	Trial 1	Trial 2	Trial 3	Trial 4	Trial 5	Average	Std. Dev.	CV
+19	725	1288	581	676	1189	**892**	**323**	**36.2**
+18	3037	5441	3950	3353	3294	**3815**	**969**	**25.4**
+17	11612	13062	11087	12534	12075	**12074**	**771**	**6.4**
+16	19676	24866	20798	21778	20105	**21445**	**2071**	**9.7**
+15	25278	33134	24837	27659	24844	**27150**	**3544**	**13.1**
+14	23581	28359	21256	24344	22353	**23979**	**2717**	**11.3**
+13	10528	13706	10328	12084	11991	**11727**	**1370**	**11.7**
+12	4305	4907	4000	4257	4305	**4355**	**334**	**7.7**
+11	2920	3034	2492	3034	3047	**2905**	**237**	**8.1**
+10	3924	3134	2873	3405	3700	**3407**	**422**	**12.4**
+9	9591	9322	7889	8800	9583	**9037**	**718**	**7.9**
+8	11487	15684	11386	12566	11514	**12527**	**1829**	**14.6**
+7	1006	1742	1231	1355	961	**1259**	**315**	**25.0**
	127670	**157679**	**122708**	**135845**	**128961**	**134573**	**13743**	**10.2**

Optics, Sturbridge, MA) and gain were used for both the four-anode and the single-anode experiments. The microchannel plates have a 40.00 mm minimum quality area, 10 μm channel diameter, 8° bias angle, and 12 μm center to center spacing.

Analyte solutions were prepared in concentrations of 0.2, 2.0, and 20 μM. All solutions were 2:1 MeOH to H_2O with 1% formic acid. Cytochrome *c* was purchased from Sigma.

Data acquisition and analysis were performed using a PC compatible computer. Acquisition control and display were done with software written for the Ionwerks TDC. Analysis was done using GRAMS/386 (Galactic Software).

Results and Discussion

To illustrate the multi-anode TDC data acquisition mode of ESI-TOF the mass spectrum of cytochrome *c* at 0.2 μM was acquired using a single-anode detector (Figure 1a) and a four-anode detector (Figure 1b). Although the overall appearance of the two spectra is similar, there are notable differences in the spectra. The abundance of all charge states increases and the signal-to-noise ratio (S/N) in the four-anode spectrum (S/N 171) is greater than twice that of the single-anode spectrum (S/N 74). Note that the abundance of the charge states less than +15 are greater in the multi-anode spectra, especially the +6 to +9 charge states. The higher abundance of the lower charge states could result from different spray conditions but the result is observed in all the data comparing the two anode configurations. This observation suggests that detector saturation is occurring for the single-anode detector. That is, counting efficiencies for TDC acquisition of ESI-TOF mass spectra can be increased by using a multi-anode detector. At 2.0 and 20 μM cytochrome *c* concentrations, the S/N ratios are approximately the same for the four-anode and single-anode spectra. The noise level at 2.0 and 20 μM in the four-anode spectra is greater than the 0.2 μM concentration and approximately four times the noise level of the single-anode spectra. The increase in noise is because of an increase in abundance of solvent ions and other chemical background ions in the four-anode experiment at 2.0 and 20 μM concentrations.

Tables 1, 2, and 3 are summations of the integrated areas of the individual charge states of cytochrome *c* at

Table 2. Integrated area of observed charge states of cytochrome *c* at 2.0 μM

Single anode	Area (Counts ∗ nS)							
Charge state	Trial 1	Trial 2	Trial 3	Trial 4	Trial 5	Average	Std. Dev.	CV
+20	203	231	216	167	162	**195.8**	**30**	**15.5**
+19	1487	1675	1741	1797	1912	**1722.4**	**158**	**9.2**
+18	6791	8128	7884	7475	7277	**7511**	**523**	**7.0**
+17	16741	18967	20992	21147	18483	**19266**	**1844**	**9.6**
+16	29287	31078	35281	34833	30039	**32103.6**	**2775**	**8.6**
+15	35855	37556	40656	40844	35364	**38055**	**2592**	**6.8**
+14	30073	32082	35223	33737	29311	**32085.2**	**2466**	**7.7**
+13	13550	15722	15068	17141	13178	**14931.8**	**1621**	**10.9**
+12	3851	4406	4431	5583	3983	**4450.8**	**682**	**15.3**
+11	1364	1312	1862	1791	1598	**1585.4**	**246**	**15.5**
+10	583	1137	1025	1219	752	**943.2**	**268**	**28.4**
+9	1360	1884	2081	2087	1550	**1792.4**	**326**	**18.2**
+8	2134	2734	3106	3642	2716	**2866.4**	**556**	**19.4**
+7	207	425	312	517	409	**374**	**118**	**31.6**
	143486	**157337**	**169878**	**171980**	**146734**	**157883**	**12985**	**8.2**
Four anode	Area (Counts ∗ nS)							
Charge state	Trial 1	Trial 2	Trial 3	Trial 4	Trial 5	Average	Std. Dev.	CV
+20	752	947	558	561	395	**643**	**212**	**33.0**
+19	7500	6775	7247	7362	7006	**7178**	**289**	**4.0**
+18	24388	24262	21169	19272	20359	**21890**	**2323**	**10.6**
+17	55606	57216	48789	47419	49547	**51715**	**4391**	**8.5**
+16	90559	87753	77917	73541	78731	**81700**	**7156**	**8.8**
+15	117295	112281	98155	97106	96159	**104199**	**9853**	**9.5**
+14	104448	100492	86361	85169	86561	**92606**	**9128**	**9.9**
+13	58530	53069	41719	43383	46887	**48718**	**7000**	**14.4**
+12	23569	20993	18931	16231	17187	**19382**	**2961**	**15.3**
+11	12361	12866	9074	8760	8805	**10373**	**2056**	**19.8**
+10	9762	9884	8625	7840	8072	**8837**	**946**	**10.7**
+9	24720	24366	21491	19994	19170	**21948**	**2514**	**11.5**
+8	37289	41647	35442	32547	35012	**36387**	**3392**	**9.3**
+7	4897	3745	3234	3206	3459	**3708**	**699**	**18.8**
	571676	**556296**	**478712**	**462391**	**477350**	**509285**	**50637**	**9.9**

0.2, 2.0, and 20 μM, respectively. Each table contains the integrated area of the cytochrome *c* charge states for the single-anode and the four-anode experiment at the respective analyte concentrations. At each concentration the integrated area is dramatically increased in the four-anode experiment versus the single-anode experiment. In some instances the number of charges states observed is increased when using the four-anode detector (see Table 1), whereas in other cases the abundance of a particular charge state is increased enough to be significant in each trial (see Tables 1 and 3).

Figure 2 contains a plot of the data from Tables 1, 2, and 3. Although both calibration curves are reasonably linear [R^2 values of 0.9897 (single anode) and 0.9977 (four anode)], the sensitivity (slope) for the two calibrations are significantly different. The slope for the four-anode curve indicates an increase in counting efficiency of the four-anode detector versus the single-anode detector. The average increase in counting efficiency for the four-anode detector is approximately 2.5 times that of the single-anode detector based on the difference of the slopes. The slopes follow the trend in the tabulated data; the offsets for the calibration curves do not coincide. Presumably, the difference is based on the higher number of background counts associated with the four-anode spectra. Crosstalk between anodes could also contribute to the higher intercept assuming the intensity of the crosstalk is greater than the discriminator setting. For this four-anode detector, the measured crosstalk between anodes is less than or equal to 10% the intensity of the primary signal. In a second generation anode, the crosstalk between anodes is less than 0.1%. Regardless of the inflated intercept, the linearity of the curve is preserved and an overall increase in abundance of detected ions is observed when the four anode is implemented.

In addition to increased counting efficiency, position sensitive detection can be accomplished with the four-anode detector and can be used as a diagnostic of ion trajectories and transmission of the ions through the TOF analyzer. For example, Figure 3 displays a blowup of the time region around the $[M+15H]^{+15}$ ion of

Table 3. Integrated area of observed charge states of cytochrome *c* at 20 μM

Single anode	Area (Counts ∗ nS)							
Charge state	Trial 1	Trial 2	Trial 3	Trial 4	Trial 5	Average	Std. Dev.	CV
+21	455	527	372	398	303	**411**	**85**	**20.6**
+20	6649	6544	5996	5708	6050	**6189.4**	**395**	**6.4**
+19	38677	42003	45749	44991	46755	**43635**	**3290**	**7.5**
+18	120691	134956	138711	140387	136016	**134152.2**	**7826**	**5.8**
+17	230125	246878	284069	282537	275922	**263906.2**	**24131**	**9.1**
+16	311725	347209	372797	373437	366754	**354384.4**	**26107**	**7.4**
+15	323175	361650	387503	388453	393650	**370886.2**	**29430**	**7.9**
+14	216216	243720	274853	279159	283103	**259410.2**	**28730**	**11.1**
+13	98222	107269	129345	126253	133434	**118904.6**	**15307**	**12.9**
+12	37184	40909	46428	47526	49747	**44358.8**	**5165**	**11.6**
+11	16506	17711	22261	23144	21419	**20208.2**	**2926**	**14.5**
+10	8311	10914	10921	11497	11812	**10691**	**1385**	**13.0**
+9	10014	12770	14125	14567	12816	**12858.4**	**1777**	**13.8**
+8	17722	20152	22234	23641	22389	**21227.6**	**2326**	**11.0**
+7	2017	2091	2094	2330	2206	**2147.6**	**122**	**5.7**
+6					232	**232**		
+5	1078	867	1132	1531	1264	**1174.4**	**245**	**20.9**
+4	211	528	363	439	687	**445.6**	**178**	**40.0**
	1438978	**1596698**	**1758953**	**1765998**	**1764559**	**1665037**	**145508**	**8.7**
Four anode	Area (Counts ∗ nS)							
Charge state	Trial 1	Trial 2	Trial 3	Trial 4	Trial 5	Average	Std. Dev.	CV
+21	1245	1047	1222	762	850	**1025.2**	**216**	**21.1**
+20	14767	11808	11623	10259	11389	**11969.2**	**1676**	**14.0**
+19	107889	80767	88898	79303	72841	**85939.6**	**13536**	**15.8**
+18	296206	258287	252236	238659	241150	**257307.6**	**23177**	**9.0**
+17	547315	532933	501645	541620	485159	**521734.4**	**27003**	**5.2**
+16	796164	730704	730187	767878	708770	**746740.6**	**34866**	**4.7**
+15	875853	843225	792295	830756	769647	**822355.2**	**41982**	**5.1**
+14	707368	683359	668242	669547	647706	**675244.4**	**22009**	**3.3**
+13	395119	363690	356354	348644	342633	**361288**	**20509**	**5.7**
+12	178488	172090	192064	176197	159187	**175605.2**	**11848**	**6.7**
+11	110770	96928	97308	93873	86083	**96992.4**	**8926**	**9.2**
+10	71606	68206	67907	67000	60312	**67006.2**	**4130**	**6.2**
+9	112572	95244	91851	99039	103341	**100409.4**	**8036**	**8.0**
+8	165494	187368	203256	234945	244166	**207045.8**	**32728**	**15.8**
+7	23990	27741	28077	32220	32655	**28936.6**	**3579**	**12.4**
+6	1328	1154	1311	1534	1716	**1408.6**	**219**	**15.5**
+5	1645	1863	1797	2672	2237	**2042.8**	**414**	**20.3**
+4	2415	2403	1506	1734	1309	**1873.4**	**512**	**27.3**
	4410234	**4158817**	**4087779**	**4196642**	**3971151**	**4164925**	**161802**	**3.9**

cytochrome *c*. Each spectrum contained in the figure is from one of the four channels of the four-anode detector. From this figure we can tell that two of the four anodes are responsible for most of the counts detected. Using this information it is possible to evaluate the trajectory of the ions from the source to the detector and optimize for a more consistent coverage of the MCP surface.

Figure 4 illustrates that the integrity of the mass resolution of the analyzer is retained in each channel of the multi-anode detection system and in the composite spectrum of the four channels. Figure 4a contains the time region of the $[M+15H]^{+15}$ ion of cytochrome *c*. The resolution of the single-anode and the signal from the sum of the four individual anodes is the same, 1000 $t/2\Delta t$ FWHM. Figure 4b contains the time region of the protonated methanol molecule $[MeOH+H]^{+}$. Again the resolution is constant for the single anode versus the summation of the four individual anodes. Thus, no compromise for resolution is taken for an increase in sensitivity.

Conclusion

Implementation of a four-anode detector in an ESI-TOF instrument produces a 2.5 times increase in counting efficiency of a TDC data acquisition system without compromising mass resolution. The multi-anode con-

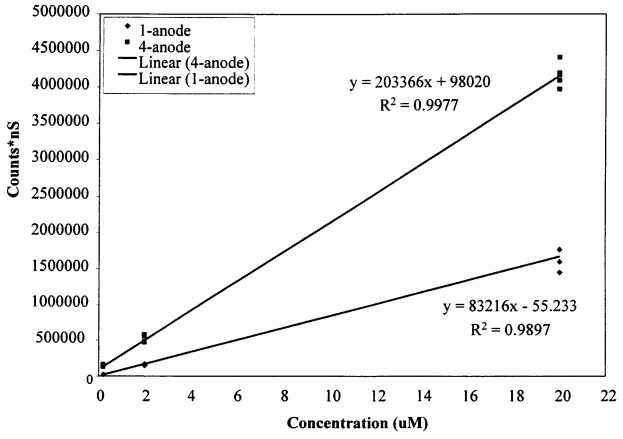

Figure 2. Integrated area vs. concentration for cytochrome *c* charge states.

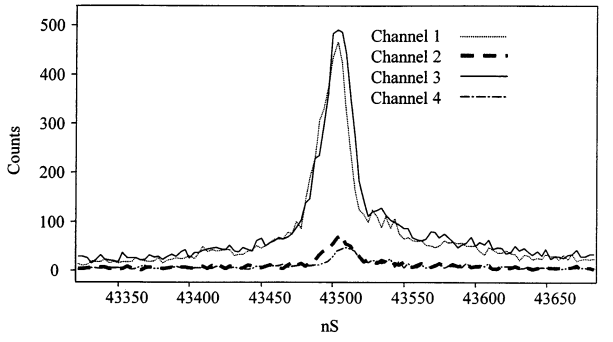

Figure 3. Expansion of the time region of the $[M+15H]^{+15}$ charge state of cytochrome *c* showing the individual channels of the four-anode detector.

figuration also serves as a diagnostic tool for optimizing ion transmission. The four-anode design is used in conjunction with a multichannel TDC data acquisition system. The multichannel data acquisition system allows for histogramming and storage of the multichannel output of the detector as a single spectrum or four individual spectra. Multiplexing the four individual signals into one spectrum allows for simple summation of the four individual signal channels. Histogramming each channel in the four channel mode provides the four individual spectra for ion transmission diagnostics.

Acknowledgments

This work was supported by grants from the Department of Energy, Division of Chemical Sciences, Office of Basic Energy Science, and the Texas Advanced Technology Program. Ionwerks would like to acknowledge and thank the NIH for support under SBIR phase I grant no. 1R43RR12059-01 A1.

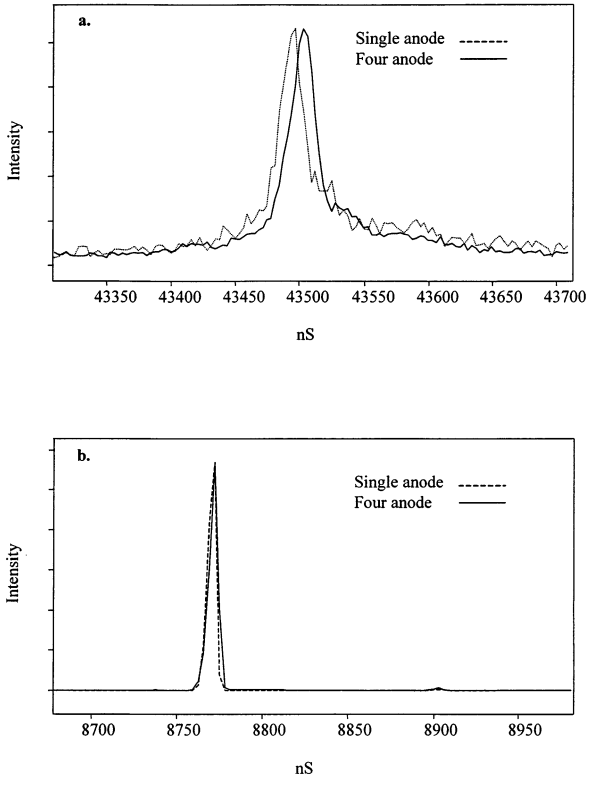

Figure 4. Time spectra from the single anode and the summation of the four anodes for **(a)** cytochrome *c* $[M+15H]^{+15}$ and **(b)** $[MeOH+H]^{+}$.

References

1. Cox, K. A.; Gaskell, S. J.; Morris, M.; Whiting, A. *J. Am. Soc. Mass Spectrom.* **1996,** *7*, 522–531.
2. Hop, C. E. C. A.; Bakhtiar, R. *Biospectroscopy,* **1997,** *3*, 259–280.
3. Bondarenko, P. V.; Watkins, L. K.; Cruzado, I. D.; Cockrill, S. L.; MacFarlane, R. D. 45th ASMS Conference on Mass Spectrometry and Allied Topics, June 1–5, 1997, Palm Springs, CA, p 1313.
4. Huang, E. C.; Pramanik, B. N.; Tsarbopoulos, A.; Reichert, P.; Ganguly, A. K.; Trotta, P. P.; Nagabhushan, T. L., Covey, T. R. *J. Am. Soc. Mass Spectrom.* **1993,** *4*, 624–630.
5. Lei, Q. P. L.; Cui, X.; Kurtz, D. M., Jr.; Amster, I. J.; Chernushevich, I. V.; Standing, K. G. *Anal. Chem.*, in press.
6. Mirgorodskaya, O. A., Shevchenko, A. A.; Chernushevich, I. V.; Dodonov, A. F.; Miroshnikov, A. I. *Anal. Chem.* **1994,** *66*, 99–107.
7. Verentchikov, A. N.; Standing, K. J.; Ens, W. *Anal. Chem.* **1994,** *66*, 126–133.
8. Pinkston, J. D.; Rabb, M.; Watson, J. T.; Allison, *J. Rev. Sci. Instrum.* **1986,** *57*, 583–592.
9. Rockwood, A. L.; Fabbi, J. C.; Harris, L.; Davis, L.; Lee, E. D.; Ogden, C.; Tolley, H.; Gunsay, M.; Sin, J. C. H.; Lee, H. G. *45th ASMS Conference on Mass Spectrometry and Allied Topics*; Palm Springs, CA, June 1–5, 1997, p 779.